https://doi.org/10.5194/egusphere-2026-3515
Preprint. Discussion started: 26 August 2026

Why does the Northwest Pacific Ocean (Kamchatka Margin) have a different carbonate time series than the rest of the Pacific? Regional carbonate production is greater than deep Pacific dissolution at the start of interglacials

Mitchell Lyle[1], Annette Olivarez Lyle

[1]College of Earth, Ocean, and Atmospheric Sciences, Oregon State University, Corvallis OR 97331 USA

Correspondence to: Mitchell Lyle (Lylem@oregonstate.edu)

Abstract

Pleistocene records of sedimentary carbonate from most of the Pacific Ocean have a strong 100-ky cyclicity, attributed for the most part to glacial-interglacial variation in carbonate dissolution. Pleistocene glacial intervals throughout the Pacific Ocean have high $CaCO_3$ burial and preservation and accelerated dissolution in interglacial intervals. Records from the equatorial Pacific, Ontong Java Plateau, Shatsky Rise, and along the California continental margin all have this pattern, attributed to changes in corrosiveness of deep waters in the Pleistocene. Surprisingly, $CaCO_3$ records from the far NW Pacific near Kamchatka (ODP Site 882 and cores nearby) have high $CaCO_3$ during early interglacial intervals and no $CaCO_3$ in the glacials, opposite to the rest of the Pacific. We synthesise evidence to suggest that sea ice and/or low salinity surface waters over Site 882 impairs glacial carbonate production sufficiently so that no $CaCO_3$ is buried during glacial intervals. $CaCO_3$ is found in sediments at the beginnings of interglacial intervals, likely because of changes in surface $CaCO_3$ production as oceans reorganize and the Bering Strait opens to shunt sea ice and low salinity water north into the Arctic. The deposition of $CaCO_3$, consistently associated with interglacial intervals at Site 882, implies that glacial sea ice and the associated low salinity surface layer was a factor affecting NW Pacific carbonate deposition during glacial-interglacial transitions throughout the Pleistocene.

https://doi.org/10.5194/egusphere-2026-3515
Preprint. Discussion started: 26 August 2026

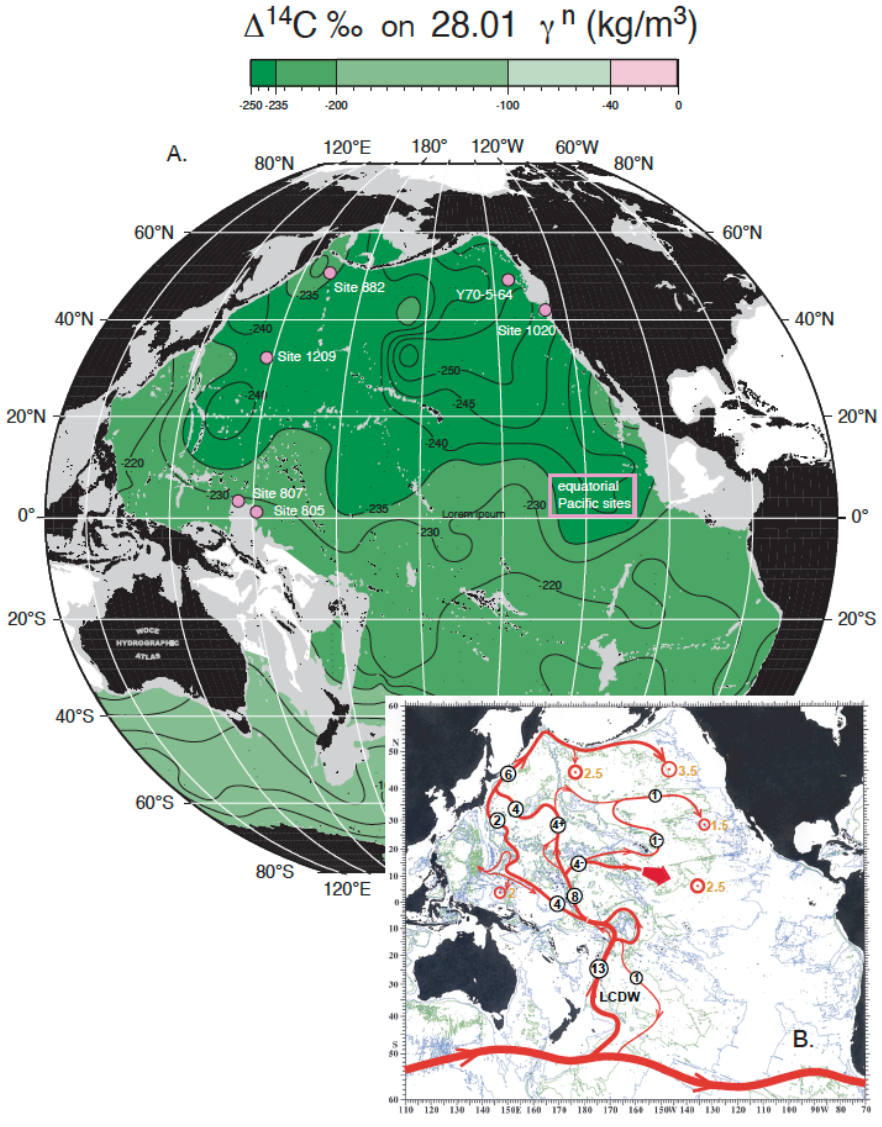

25 ***Figure 1: (a) Location of cores discussed in this paper. Sites 805, 807 (Ontong Java Plateau, Yasuda et al, 1993; Zhang et al., 2007) and Site 1209 (Bordiga et al., 2013) are records that explore dissolution indices on glacial-interglacial scales. All North Pacific sites are within the boundary zone between Pacific Deep Water (PDW) and Lower Circumpolar Deep Water (LCDW), as defined by Talley et al (2007). The sites' locations are displayed on a map of the $\Delta^{14}C$ at the depth of the 28.01 kg/m^3 neutral density surface (WOCE Atlas V. 2, http://whp-atlas.ucsd.edu/pacific/map_isopycnals.htm), which marks the***
30 ***lower surface of PDW and are where the cores are located. Cores in the equatorial Pacific lie within the mixing zone of PDW and eastward flow of LCDW.***

https://doi.org/10.5194/egusphere-2026-3515
Preprint. Discussion started: 26 August 2026

1 Introduction: Anomalous $CaCO_3$ records in the NW Pacific

Cyclic carbonate ($CaCO_3$) burial is a hallmark of pelagic sediment records recovered from above the carbonate compensation depth (CCD) throughout the oceans. The sedimentary records mark an interplay between carbonate production at the surface of the ocean and dissolution at the sea floor where pressure, temperature, and the buildup of dissolved inorganic carbon (DIC) combine to make carbonates more soluble. Cyclicity is introduced by changes in ocean carbonate chemistry coherent with glacial cycles. Changes in abyssal carbonate chemistry with the Pleistocene glaciations imposes a common signal upon cores thousands of kilometers apart. In most of the Pacific, glacial intervals are characterized by sediments with high $CaCO_3$ contents and interglacial periods with low $CaCO_3$ (Arrhenius, 1952; Hays et al., 1969; Farrell and Prell, 1989)). The same pattern of preservation and dissolution as is found in the equatorial Pacific also is found on Ontong Java Plateau (Yasuda et al., 1993; Zhang et al., 2007), Shatsky Rise (Bordiga et al, 2013), and in the northeast Pacific (Zahn et al, 1991; Karlin et al, 1992, Lyle et al., 2000).

The flow of Pacific abyssal waters links carbonate dissolution through a common carbon chemistry (Fig 1). There is no evidence that Pacific deep-water flow paths changed in the glacial intervals of the Pleistocene. The observed abyssal flow begins as a separation from circumpolar deep-water flow to the east of Australia, that flows north in the western Pacific, east across the North Pacific, and then south along the California Margin to the equatorial Pacific. Finally, these waters flow across the sediments of the eastern and central Pacific and back to the Antarctic along the western margin of the east Pacific Rise. Kawabe and Fujio (2010) estimate that 12 Sv (10^6 m^3/s) of lower circumpolar deep water (LCDW) flows north of the equator into the deep Northwest Pacific, and roughly 4 Sv flow eastward south of Hawaii to mix with Pacific Deep Water (PDW) returning from the northeast Pacific. LCDW upwells and mixes with upper Circumpolar Deep water to form Pacific Deep Water (PDW) north of Hawaii, of which 13 Sv flows southeast past Hawaii east of 140°W and out of the NE Pacific Basin. All the sites discussed in this paper are in PDW and should have a common dissolution imprint.

The equatorial Pacific, located within the returning abyssal flow from the North Pacific, has long been known to have characteristic Pleistocene carbonate cycles (Arrhenius, 1952; Hays et al, 1969; Farrell and Prell,1989), characterized by high $CaCO_3$ in glacial intervals and low $CaCO_3$ in interglacial intervals. In the shallower eastern equatorial Pacific, Hagelberg et al. (1995) also found that there was also a strong precessional variation to $CaCO_3$ deposition, while the obliquity and eccentricity signals were present but weaker. Hagelberg et al. (1995) attributed the high precessional signal to $CaCO_3$ production, since the signal is strongest at the equator. Nevertheless, Lyle et al. (2019) using CaCO3:$BaSO_4$, an indicator of relative preservation of $CaCO_3$ in the sediments, found a strong eccentricity link from 1600 ka onward, marking changes in dissolution. In the western Pacific on the elevated topography where carbonate is preserved, evidence of heightened dissolution in the interglacial periods is marked by higher foraminiferan dissolution indices on the Ontong Java Plateau (Site 805, Yasuda et al., 1993; Site 807, Zhang et al., 2007) and on Shatsky Rise by nannofossil dissolution indices (Bordiga et al.,2013).

https://doi.org/10.5194/egusphere-2026-3515
Preprint. Discussion started: 26 August 2026

Northeast Pacific 100 kyr cycles are like those of the equatorial Pacific (Zahn et al, 1991; Karlin et al, 1992, Lyle et al, 2000). Variable dissolution correlated with eccentricity defines the long-term equatorial sedimentary carbonate record and most records of the pelagic Pacific (Fig 2). This common signal links $CaCO_3$ records in most of the deep Pacific.

Only one area, in the far NW Pacific near Kamchatka, has a different time series, with well-documented $CaCO_3$ records where highest $CaCO_3$ is found in the early parts of interglacial intervals (Keigwin et al., 1992; Haug et al., 1995). This paper studies why the far NW Pacific, as epitomized by Site 882, has different $CaCO_3$ time series than the rest of the Pacific basin.

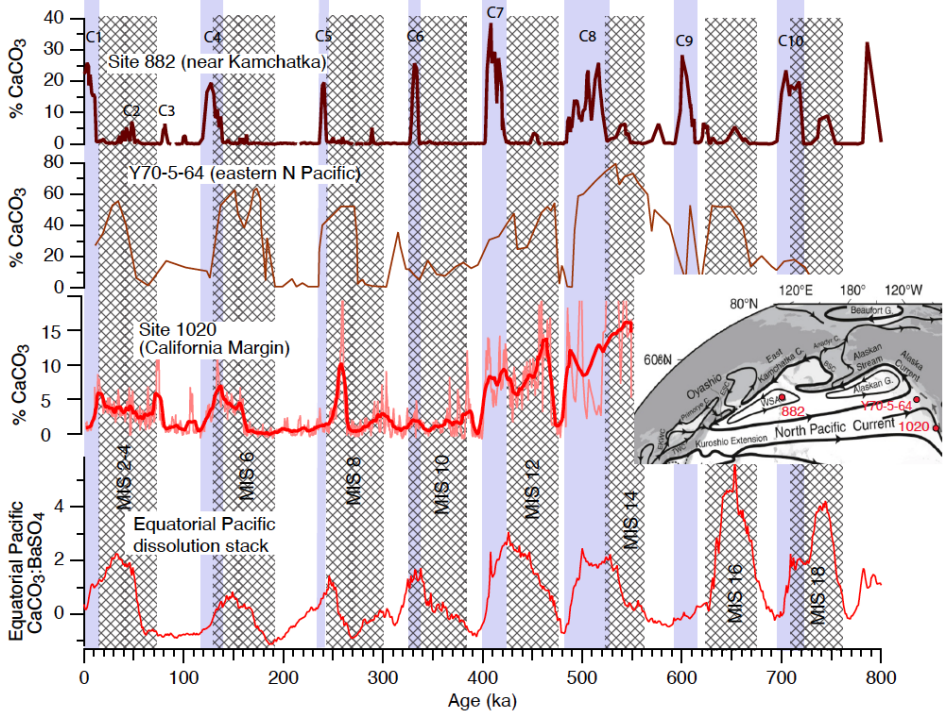

Figure 2: Carbonate profiles from the North Pacific and equatorial Pacific. Lavender shading marks peaks in Site 882 $CaCO_3$ content. High $CaCO_3$ intervals are numbered as in Table 1 and mostly occur at the beginnings of interglacial intervals. Gray crosshatching marks Marine Isotope Stage (MIS) glacial intervals (Lisiecki and Raymo, 2004), which occasionally overlap slightly with $CaCO_3$ intervals from Site 882. Inset and Fig 2 show locations of the North Pacific cores on the surface circulation of the North Pacific from Talley et al. (2011). Data displayed are for Site 882: this study and Haug, 1995; Y70-5-64: Zahn et al., 1991 (Table S7); Site 1020: Lyle et al. 2000 [all data, light line and a smoothed record, bold line]. The equatorial stack of $CaCO_3$:$BaSO_4$ is a measure of carbonate dissolution relative to production in the equatorial Pacific region (Lyle et al., 2019). High $CaCO_3$: $BaSO_4$ indicates low dissolution.

https://doi.org/10.5194/egusphere-2026-3515
Preprint. Discussion started: 26 August 2026

1.1 Anomalous $CaCO_3$ deposition near the Kamchatka margin

While most Pacific records have high $CaCO_3$ contents associated with glacial intervals (the even-numbered MIS intervals, Fig 2), Site 882 and nearby shorter records from piston cores (Keigwin et al, 1992; Haug et al, 1995, Haug, 1995, Keigwin, 1998) have little or no carbonate in glacials and a $CaCO_3$ peak primarily within early interglacial periods.

Haug et al. (1995) analysed both the $CaCO_3$ and bio-SiO_2 records from Site 882 on Detroit Seamount for the last 6 million years and showed that the carbonate cycles in the far NW Pacific are nearly opposite those of the equatorial Pacific since the initiation of Northern Hemisphere glaciation. Haug et al. (1995) also suggested that surface production must have driven the signal but did not dig deeper. Here we will investigate the production hypothesis in more detail and will test which surface environmental conditions likely drove changes in carbonate production, e.g., changes in upwelling, surface sea-ice and salinity, or summer sea surface temperatures (SST) control of coccolithophorid carbonate production.

What makes the Kamchatka margin different? The alternate hypothesis to surface production for an alternate $CaCO_3$ time series in the NW Pacific is that deep circulation to the Kamchatka margin is different from that of the rest of the Pacific. If this were true, there should be a separate deep flow to the Kamchatka margin relative to the rest of the Pacific. However, there is no evidence that there is a separate flow that could reach the NW Pacific. Deep waters over Site 882 are the same as those in the rest of the Pacific basin (Fig 1B), as discussed later.

There are significant differences between the eastern and western subarctic Pacific which might affect carbonate production (Fig 2, Talley et al, 2011). The modern North Pacific subpolar gyre is separated into two portions: the Western Subarctic Gyre (WSAG) that flows south along the Kamchatka margin and where Site 882 is located, and the Alaska Gyre in the eastern Gulf of Alaska. The modern WSAG receives colder, fresher water flowing out of the sea-ice-forming regions in the Bering Sea and Sea of Okhotsk and may have received more low salinity water from sea-ice formation during glacial intervals. In contrast, the eastern subarctic gyre receives northward flow from the west wind drift that crosses the Pacific at around 40°N, so is represented by the bulk properties of the North Pacific. Hence, we note the far northwestern Pacific has unique regional oceanography that may explain the differences in carbonate burial that have been observed.

1.2 The Bering Straits hypothesis for Kamchatka Margin $CaCO_3$ burial.

If changes in production of $CaCO_3$ in surface waters causes the anomalous $CaCO_3$ record along the Kamchatka margin, something must suppress or promote the growth of calcareous nannoplankton, since most $CaCO_3$ is produced by them. Coccolithophores are strongly controlled by water masses in the subarctic (Samtleben et al., 1995). Conditions that could suppress calcareous nannoplankton growth include low temperature, relatively fresh cold surface water (Bendle et al., 2005), and competition between calcareous nannoplankton and diatoms for nutrients and sunlight (Dymond and Lyle, 1985).

https://doi.org/10.5194/egusphere-2026-3515
Preprint. Discussion started: 26 August 2026

While we will investigate all these hypotheses, much of the evidence presented later points to regional intrusion of relatively cold fresh surface seawater with some sea ice during glacial intervals that suppressed $CaCO_3$ production. Conversely, relatively high $CaCO_3$ burial occurs when the region is covered by more saline surface water typical of the rest of the North Pacific. One hypothesis that links $CaCO_3$ burial to early interglacial periods on the Kamchatka margin is shown in Figure 3. Assuming that $CaCO_3$ production was suppressed by the presence of sea ice and accompanying cold relatively fresh surface sea water, periods of $CaCO_3$ burial mark intervals when water more typical of the North Pacific occupied the region and the cold fresh sea-ice-filled surface waters went elsewhere.

$CaCO_3$ deposition is correlated to the initial opening of the Bering Strait over many deglaciations (Fig 3). and thus, may represent a significant transfer of ice-filled low salinity water from the Bering Sea into the Arctic Ocean and the North Atlantic. Modern flow through the Bering strait has been reported as 0.8 $x10^6 m^3$/sec (Woodgate and Aagaard, 2005), although modelling and recent measurements find that throughflow is now ~1.0 $x10^6 m^3$/sec (Yang and Cessi, 2024; Woodgate, 2018) and has increased from 0.8 $x10^6 m^3$/sec since 2002.

The opening of the Bering Strait has significant global climate impacts within models, primarily because water flows from the Pacific, through the Arctic, to the North Atlantic. The modelling has shown that initial flow through the Bering Strait strongly affects deep water production in the North Atlantic by adding low salinity water to the North Atlantic and suppressing the formation of deep water (Hu et al., 2010, 2015). Cessi (2020) also shows via an idealized model, that the strength of flow through the Bering strait depends on the sea surface height difference between the Pacific and North Atlantic, a transfer that may slow as sea levels rise and the interglacial advances. In this case, the $CaCO_3$ deposition reflects higher calcareous nannofossil production of $CaCO_3$ in North Pacific seawater relative to that in less saline (and perhaps more ice-ridden) waters of surface waters near the ice edge.

https://doi.org/10.5194/egusphere-2026-3515
Preprint. Discussion started: 26 August 2026

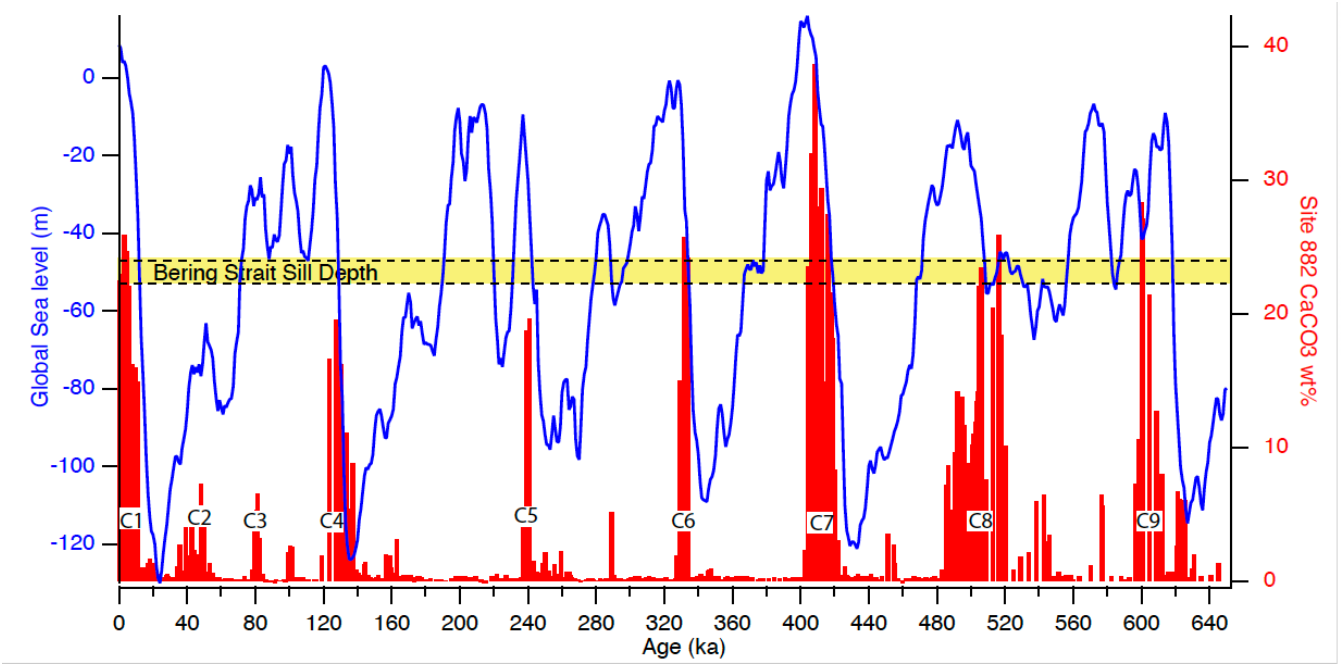

Figure 3: Comparison of high $CaCO_3$ intervals at Site 882 with changes in sea level from Spratt and Lisiecki (2016). Yellow banded interval marks the sill depth range of Bering Strait (53-47 m; Jakobsson et al., 2017). The high $CaCO_3$ intervals are apparently associated with the rapid rise in sea level that opens the Bering Strait connection to the Arctic Ocean.

High $CaCO_3$ at Site 882 and other sites along the Kamchatka margin occur early in interglacial intervals (Fig 2). The Site 882 deposition spikes typically begin when sea level rise first connects the Pacific and the Arctic basins through the Bering strait (Fig 3). Jakobsson et al. (2017) established a 53 m depth in the Bering Strait and 47 m depth at north and south entrances, which is used as the range in Bering Strait sill depth in figure 3. Jakobsson et al (2017) and Pico et al (2020) both establish that during the last deglaciation, the strait flooded during the Melt Water Pulse 1b event (11.5-11.1ka, Abdul et al, 2016).

We highlight two important points elucidated from sedimentary evidence by Haug et al. (1999), Kotilainen and Shackleton (1995), McClymont et al (2008), Martinez-Garcia et al (2010), and Jaccard et al (2005, 2009). The first is that lower salinity water inhabited the region during glacial intervals; and second, both productivity and diatom burial varied significantly. We take this information to explore why the carbonate depositional time series is so different from those of the other biogenic sediment components, and why the NW Pacific differs so strongly from the NE Pacific and the equatorial Pacific region.

https://doi.org/10.5194/egusphere-2026-3515
Preprint. Discussion started: 26 August 2026

2 Methods

We investigated the biogenic deposition for the last 650 kyr at ODP Site 882 by collecting new data for particulate organic carbon (POC) and $CaCO_3$ from the top 32 meters composite depth of the spliced continuous sediment section. We also calibrated the gamma ray attenuation (GRA) bulk density record to discrete biogenic-SiO_2 measurements following the suggestion of Kotilainen and Shackleton (1995). We checked the shipboard sediment splice, adding depth registered core images to confirm the continuous sediment interval. We found one significant discrepancy in the splice interval but was able to correct it and readjust the affected depths to the new splice and ultimately corrected the age model to include the new (corrected) sediment interval. The adjustment occurs at ~360 ka in this paper's age model.See the supplemental material for illustrations and the revised splice

2.1 Sediment splice and age model

We reviewed the shipboard sediment splice and adjusted it based not only on the shipboard MultiSensor Track (MST) physical properties data but also using core sediment images extracted from the core photos archived at IODP Gulf Coast Repository (http://iodp.tamu.edu/janusweb/imaging/photo.shtml) . The core sediment images were extracted from the core photos using CODD 2.1 software (Code for Ocean Drilling Data, https://www.codd-home.net/; Wilkens et al, 2017) and spliced into a continuous sediment column to compare with the sedimentary data. We noticed immediately that all but one high $CaCO_3$ interval matched intervals of light sediment shades typical for relatively high carbonate-containing sediments. By comparing the core images, we found that a 48 cm section of low $CaCO_3$ sediment had been erroneously omitted from the shipboard composite section in the core 882B-03H. This missing 48 cm was added, and the splice adjusted so that light-colored sediments and high carbonate data matched in both holes. The added section had low $CaCO_3$ and has an age of 358-362 ka. We did minor revisions down the sediment section and revised the splice such that most of the data previously collected by Haug et al (1995) was still in the composite splice sediment interval. The revised splice-interval tables are presented as Supplemental Table S1. Core offsets (revised depth to match features in each core) used to align cores in Holes A and B are in Supplemental Table S2.

For the most part we used the age model of Tiedemann and Haug (1995) but we calculated mildly revised ages for the interval that we added in core 882B-03 which produced higher sedimentation rates for that interval. Ages above and below the revised section were assumed correct, and the ages within the adjusted or modified or corrected interval were interpolated based upon the new depths. Sedimentation rates were then recalculated with the new age model. The new age model is listed in Table S3, along with sedimentation rates, GRA values, estimated bio-SiO_2 from the GRA, bulk MAR and bio-SiO_2 MAR.

https://doi.org/10.5194/egusphere-2026-3515
Preprint. Discussion started: 26 August 2026

2.2 Carbon analysis

Both POC and $CaCO_3$ data reported here follow the analytical protocol elucidated in Lyle et al (2000) and is based on two separate analyses of the sediment sample from the same interval. The first aliquot of the freeze-dried and powdered sediment sample is analysed for its total carbon content (POC plus C_{CO3}) in which the sediment is combusted at 1000°C with an ultra-pure oxygen carrier gas. The resulting gas generated by sediment combustion is then cleaned via scrubbers to remove water, NO_x, and chlorine from salts, and then analysed for its CO_2 content using a UIC Inc. Model CM-5012 coulometer. Likewise, the organic carbon fraction is measured from a second aliquot of sediment which first has been treated with dilute HCL before analysis to dissolve and remove the CO_2 attributed to sedimentary carbonates. The residual organic carbon fraction remaining in the aliquot is then measured in a similar manner by coulometry. The calcium carbonate carbon fraction can thus be calculated from the difference between the total carbon and organic carbon (POC) measurements, multiplied by 8.33 to convert C to $CaCO_3$. We checked for consistency of our carbon analyses, as described in Olivarez Lyle and Lyle (2005), by running an in-house sediment standard "Midway" with each carbon run and for which hundreds of analyses and summary statistics have been compiled ("Midway" standard: Total carbon = 2.64±0.02 wt %, n=523; POC = 0.85±0.01, n=570). We also analyzed every 4th unknown sample twice to monitor consistency of replication during each run. We monitor both total carbon and organic carbon. The average absolute difference between repeated unknown samples for POC is <0.01 wt%, and if this difference exceeded 0.02 wt % we re-analyzed the sample in future runs.

Samples were taken at 10 cm intervals using the shipboard splice as a guideline: for a total of 390 samples: 258 from Hole 882A and 132 samples from Hole 882B. The new POC and $CaCO_3$ data are listed in Supplemental Table S4. The $CaCO_3$ data we generated were interleaved with Haug et al. (1995) 30-cm spaced data and plotted together in Figure 4. We found little difference between the Haug et al (1995) data and ours, except that caused by the difference in sample spacing. High $CaCO_3$ intervals are numbered in Table 1 with their estimated ages.

2.3 Biogenic Opal analysis and creation of the time series

A set of samples were analysed for biogenic opal (bio-SiO_2) and then used to calibrate the GRA bulk density record as was done by Kotailenen and Shackleton (1995), who first showed that variations in the GRA density record at Sites 882 and 883 reflect changes in sedimentary bio-SiO_2. We use the term bio- SiO_2 because we report only the SiO_2 value and do not try to estimate the bound water associated with biogenic opal.

First, we analyzed discrete samples for biogenic opal (bio-SiO_2) following the protocols elucidated in Olivarez and Lyle, 2002. Samples were taken at 10 cm spacing from two intervals, from 0 to 9.335 meters composite depth (MCD) and from 21.945 to 28.145 MCD using the revised splice depth scale (Table S3). The samples were freeze-dried, ground in an aluminum oxide

https://doi.org/10.5194/egusphere-2026-3515
Preprint. Discussion started: 26 August 2026

mortar and pestle, and stored in air-tight plastic containers lined with indicating Drierite until analysis. Around 20-50 mg of dried sample was weighed, treated with H_20_2 to remove organic coatings, then HCL to remove carbonate. Finally, the sample was treated with 2-M Na_2CO_3 in a heated shaking water bath to dissolve biogenic silica. The dissolved silica was analyzed using a HACH Model DR/4000 UV-VIS spectrophotometer (Olivarez Lyle and Lyle, 2002) following the HACH Method 8186. The samples from Site 882 did not need the harsher KOH dissolution treatment because they are geologically young and contain primarily diatoms so dissolved well in Na_2CO_3. Furthermore, the Na_2CO_3 treatment is much less corrosive to volcanic glass, a persistent sedimentary component in the NW Pacific that overestimates the targeted bio- SiO_2 component. The data are reported in Table S3 as "bio-SiO_2" without any correction for bound water that may be found in biogenic opal.

In contrast to our CaCO3 data, we did not combine our bio- SiO_2 results with those reported by Haug et al (1995) for the relevant intervals. Although the two data sets are broadly similar, the Haug et al (1995) data were determined by a different analytical method (gravimetric), and were generally noisier and offset from our data. Furthermore, the variation in our leach-determined bio-SiO_2 best matched the bulk density variation in the GRA record to suggest our data overall are more accurate.

The two intervals of discrete analyses were used to calibrate the GRA wet bulk density profile for the Site 882 sedimentary splice (Figure 4). We estimated bio-SiO_2 assuming that no bio-SiO_2 was present in a sample when sediments had a GRA density ≥1.57 g/cm^3, while a sample of 100% bio-SiO_2 has a GRA density equivalent to 1.08 g/cm^3, equivalent to a porosity of 97% and an opal grain density of 2.2. These density parameters were chosen to best match the discrete bio-SiO_2-GRA comparison. Supplemental Table S4 has the estimated bio-SiO_2 data, along with the age model and bio-SiO_2 MAR data.

2.4 Mass Accumulation Rates (MAR)

Mass accumulation rates (MAR) are calculated to disentangle changes in sediment composition from changes in each components' rates of burial over a given time interval. Studying only the weight per cent data of a particular component has limited use because downcore trends may simply reflect dilution by high deposition of another, or other, sedimentary component(s). For any sedimentary interval, Multiplying the dry bulk density (DBD) by the sedimentation rate for that interval yields the bulk MAR for all components, in units of g/cm^2/kyr. Then, the bulk MAR, multiplied by the relative fraction (%/100) of any particular sedimentary component yields that component's MAR as g/cm^2/kyr. We used the Haug et al (1995) conversion from GRA density to dry bulk density (DBD=1.67*GRA-1.89) to convert the GRA record to DBD. We then used the Haug et al (1995) sedimentation rate, with our minor revision over core 882B-03 to calculate a bulk MAR. Bulk MAR, along with MARs for individual biogenic components are shown in Figure 5.

https://doi.org/10.5194/egusphere-2026-3515
Preprint. Discussion started: 26 August 2026

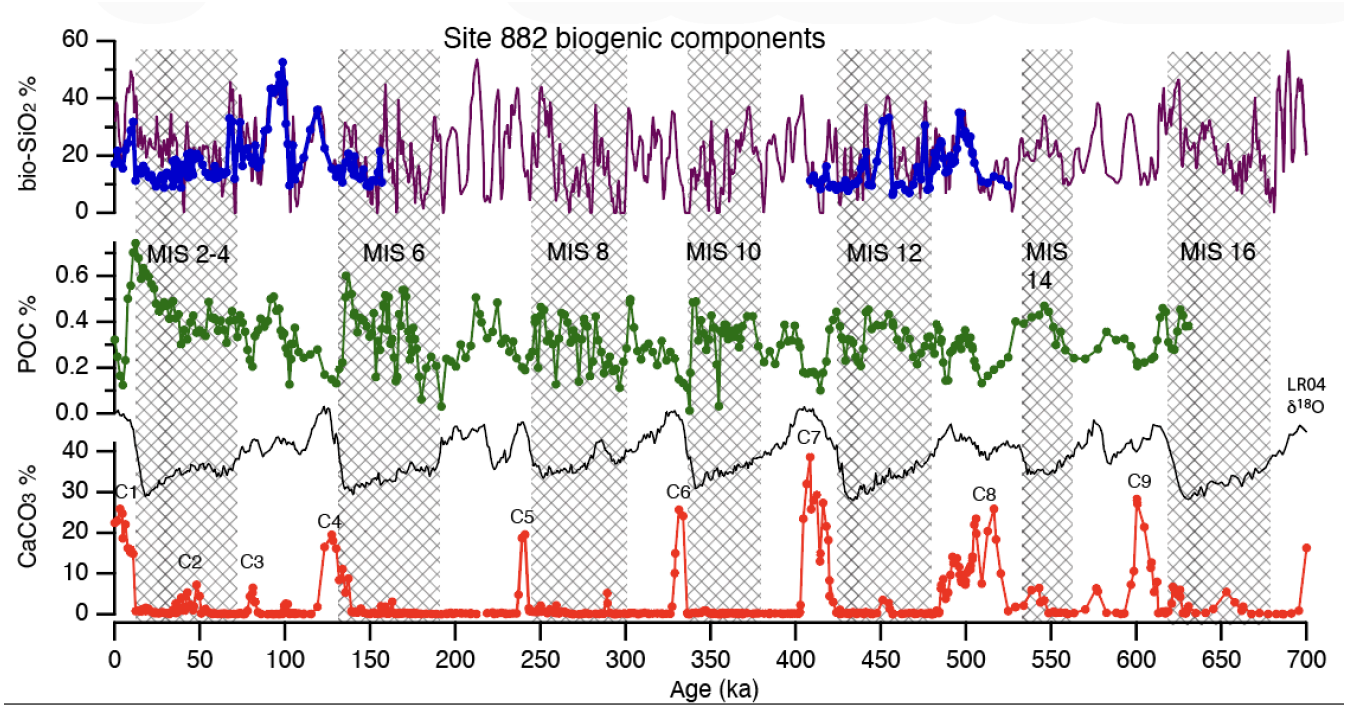

245 ***Figure 4: Biogenic contents of Site 882 sediment vs. age, using the Tiedemann and Haug (1995) age model as modified in this paper. Bio-SiO_2 contents are presented where blue data are discrete bio-SiO_2 analyses superimposed on the lavender estimate from the GRA wet bulk density record. POC (Particulate organic carbon) contents are the green record. Interglacial stages are highlighted in crosshatch and are based on the Lisiecki and Raymo (2005) stack, LR04. $CaCO_3$ (red) tends to be high at the beginnings of interglacial intervals and correlated to low POC. High $CaCO_3$ intervals, C1 thru C9,***
250 ***are labelled as in Fig 2 and Table 1.***

3 Results

The additional analyses we performed added new data for particulate organic carbon (POC) content, bio-SiO_2 (using a leach-based bio-SiO_2 % to calibrate a GRA based estimate), and we filled in data in the $CaCO_3$ profile. The new sampling and analyses produced a data set with approximately 2 kyr sample spacing, sufficient to resolve orbital cyclicity and to detect rapid
255 changes. All weight % data are shown in Figure 4, plotted against age.

3.1 Biogenic sediment components

The bio-SiO_2 data have a very strong precessional variability. Tiedemann and Haug (1995) used the precessional component of the 65°N summer insolation as a target to tune their low-resolution age model using GRA, because GRA apparently has
260 high variance at the precession periods. Since the GRA signal reflects variation in bio-SiO_2 content, bio-SiO_2 has a strong

https://doi.org/10.5194/egusphere-2026-3515
Preprint. Discussion started: 26 August 2026

precessional signal. In the 0-1 Ma interval, the bio-SiO_2 precession signal is significantly stronger than the 100 kyr Milankovitch band (Tiedemann and Haug, 1995). Obliquity variance, in contrast, is stronger than precession between 2.7 and 1 Ma. The precessional signal in bio-SiO_2 thus dominates in the 0-625 ka data presented here.

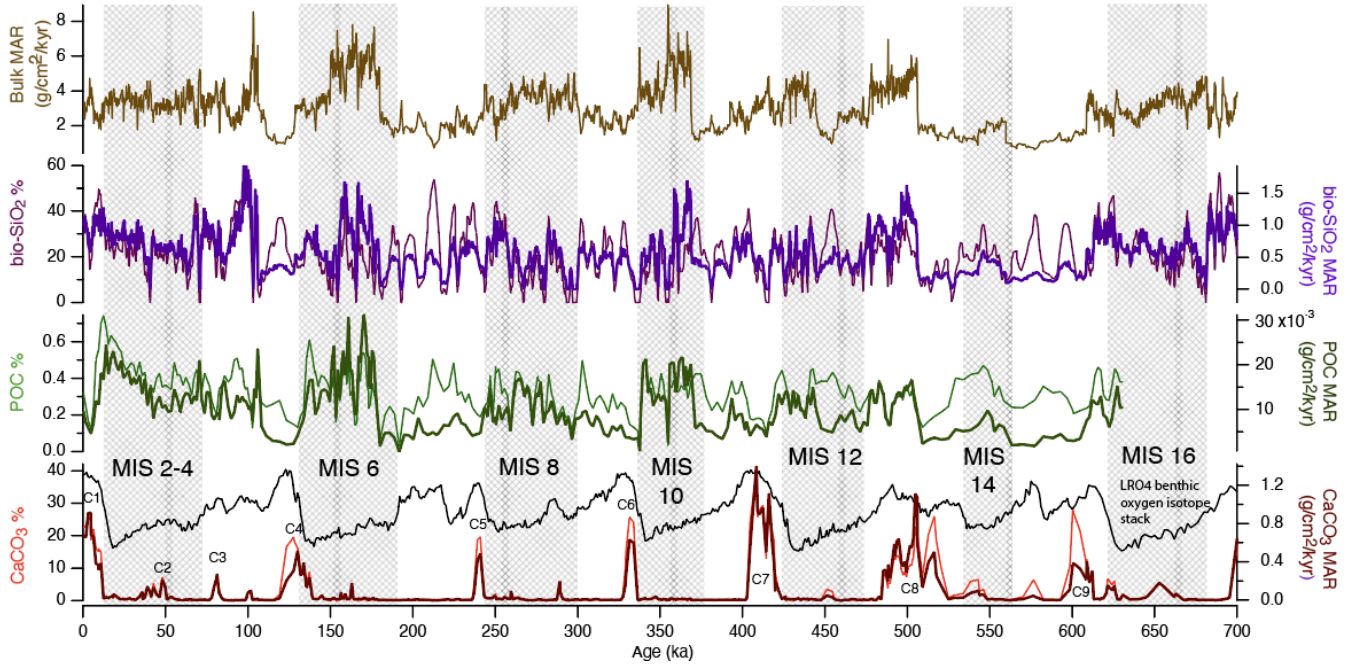

Figure 5: Mass Accumulation Rates (MARs) for bulk sediment and for biogenic components. For bio-SiO_2, POC, and $CaCO_3$, the percentage data are plotted as thin lines, and the MAR data are plotted as thick ones. The Lisiecki and Raymo (2005) isotope stack is plotted as a black line and was used to define the interglacial intervals. Precessional rhythms are reduced in the MAR data but still can be found in the bio-SiO_2 MAR. High $CaCO_3$ intervals are labelled as in Fig 2 and Table 1.

The POC contents are relatively high for a pelagic site, averaging 0.33%, with 97% of the data falling in the range between 0.1 and 0.6 %. POC. Typical POC in the equatorial Pacific in the Pleistocene, for example, is 0.12% (Lyle and Olivarez Lyle, 2024). Bio-SiO_2 and POC appear to covary, but cross-spectral analysis does not find significant coherence between them in the Milankovitch bands. Nevertheless, peaks in bio-SiO_2 content are often peaks in POC content. The beginnings of interglacial periods for the entire record tend to be characterized by low POC (Fig 4). Some relationship between bio-SiO_2 and POC should be expected because diatom primary production concurrently produces POC and bio-SiO_2, and large diatom tests help to sweep POC to the ocean floor (Ragueneau et al, 2000; Moriceau et al, 2018; Treguer et al, 2018). The lack of a strong signal between POC and bio-SiO_2 may result from changes in deep water oxygen content affecting the preservation of POC in the sediments (Jaccard et al, 2009, 2010), as discussed later.

https://doi.org/10.5194/egusphere-2026-3515
Preprint. Discussion started: 26 August 2026

$CaCO_3$ contents in the record appear as intermittent $CaCO_3$ spikes among intervening bio-SiO_2 -rich clays (Haug et al, 1995). Table 1 lists the events we tabulated through 722 ka. High $CaCO_3$ intervals typically have ~20% $CaCO_3$ and are resolved by multiple discrete measurements in the data set here (Figure 4). Rarely does the entire interglacial interval have high $CaCO_3$. Instead, high peaks appear at the initiation of the interglacial interval, occasionally with a small secondary peak later in the stage. High $CaCO_3$ contents typically coincide with the low POC intervals at the beginning of interglacial intervals. The interglacial $CaCO_3$ depositional spikes at Site 882 occur within intervals that last between 10 to 40 kyr (Table 1). However, $CaCO_3$ deposition intervals are only preserved at the very start of the interglacial interval, but do not typically persist throughout the interval.

Table 1 High CaCO3 intervals at Site 882 with their age and duration

Event number	Event Start (ka)	Event end (ka)	Interval length (kyr)
C1	12.3	0	12.3
C2	51.1	32.2	18.9
C3	85.8	75.8	10
C4	139	119.1	19.9
C5	245.3	236	9.3
C6	336.3	326.3	10
C7	423.9	402.5	21.4
C8	524.8	481.4	43.4
C9	613.9	592.9	21
C10	722	695	27

3.2 Biogenic Mass Accumulation Rates (MARs)

The time series for the bulk sediment- and biogenic- Mass Accumulation Rates (MAR) are shown in Figure 5 along with the LR04 benthic oxygen isotope stack (Lisiecki and Raymo, 2005). High bulk MAR is typical of glacial intervals, except for an interval in interglacial MIS 13. Bio-SiO_2 MARs typically comprise only 1/3 to 1/2 of the bulk MAR, indicating elevated deposition of aluminosilicates in glacial intervals. Higher glacial aluminosilicate MARs may result from regional exposure and erosion of nearby continental shelves.

Bio-SiO_2 weight percent variation has a strong precessional beat but multiplication by bulk MAR yields a tendency for higher glacial bio-SiO_2 MAR, particularly in MIS 6 and 10 (Fig 5). There is some correlation between bio-SiO_2 MAR and POC MAR, in part caused by multiplying each percent series by a common bulk MAR. Highest bio-SiO_2 MAR typically matches periods of high POC MAR, especially in MIS 13, 10, and 6, as expected if diatoms are a major component of surface producers and if diatom rain is an important mechanism to sweep POC out of the euphotic zone and bury it in the sediments (Ragueneau

https://doi.org/10.5194/egusphere-2026-3515
Preprint. Discussion started: 26 August 2026

et al, 2000; Moriceau et al, 2018; Treguer et al, 2018). There are intervals where they do not match well, as in the last half of MIS 5 where bio-SiO_2 MAR is high, but POC MAR is modest.

$CaCO_3$ deposition is intermittent, typically occurring at the beginning of interglacials, associated with both low POC % and POC MAR. $CaCO_3$ % and $CaCO_3$ MAR have similar profiles, because $CaCO_3$ deposition is intermittent, typically when bulk MAR is relatively low. High productivity is not the factor that leads to high carbonate contents in the Site 882 sediment column, nor is there better $CaCO_3$ preservation in glacials. $CaCO_3$ MAR maxima are strongly associated with POC MAR minima at the beginning of interglacial intervals. These POC MAR minima are sometimes aligned with the oxygen isotope-defined beginning of the interglacial, but are often offset (Fig 5, see MIS 7, 11, and 15). The one anomalous $CaCO_3$ MAR is in the interglacial MIS 13. It increases during the middle of the interglacial, not at its beginning. However, the MIS 13 carbonate deposition is also at the end of an extended low deposition interval and may result from anomalous deposition and enhanced preservation as sedimentation rates increased.

4 Discussion: The Anomalous $CaCO_3$ cycle near the Kamchatka Margin

Earlier studies have shown that there is a 100-kyr beat to $CaCO_3$ burial in the North Pacific from the tropics to at least 50°N in the NE Pacific (Fig 2; Farrell and Prell, 1989; Zahn et al, 1991; Karlin et al, 1992; Lyle et al, 2000, Lyle et al, 2019). In contrast, the corner of the NW Pacific near Kamchatka has a spiky signal as $CaCO_3$ is preserved and buried primarily at the beginnings of interglacial intervals. Others have proposed that changes in $CaCO_3$ production or abyssal $CaCO_3$ saturation must have caused the "Kamchatka" type of carbonate profile (Haug et al., 1995, Jaccard et al., 2005,2009) but have not explored the implications of the carbonate profiles. We synthesize evidence to show that the spiky interglacial $CaCO_3$ record marks depression of glacial $CaCO_3$ production when at least some sea ice as well as low salinity surface waters were present.

We explore whether higher surface productivity alone is the dominant factor to cause the $CaCO_3$ deposition or whether additional factors peculiar to production of $CaCO_3$ in the surface ocean might play a role as well. Much of the high productivity (monitored by the deposition of Ba) is associated with high diatom (bio-SiO_2) deposition but often without high $CaCO_3$ deposition. Other factors are apparently critical for high $CaCO_3$ production and burial.

4.1 Evidence of specific $CaCO_3$ production anomalies

Typically, we expect a proportionality between $CaCO_3$ particulate rain and export productivity (POC rain caught in sediment traps), as was observed in the equatorial Pacific and Indian Ocean JGOFS sediment trap experiments (Honjo et al, 1995,1999; Lyle and Baldauf, 2015). There is also a seasonal correspondence of high $CaCO_3$ particulate rain with high POC rain in sediment traps in the Atlantic subtropical gyre and the northeast subarctic Pacific (Conte et al, 2001; Wong et al, 2002) and in

https://doi.org/10.5194/egusphere-2026-3515
Preprint. Discussion started: 26 August 2026

the NW Pacific (Honda et al. 2002). The nearest sediment trap array to Site 882 (KNOT, Honda et al, 2002) has a modern pattern in a 3-year deployment of relatively constant $CaCO_3$ flux but with increased opal deposition in spring/summer. Highest POC deposition relative to $CaCO_3$ occurred during periods of high opal deposition. Nevertheless, under conditions of unvarying dissolution at the sea floor, higher $CaCO_3$ MAR in a time series implies an interval of higher surface productivity. When a $CaCO_3$ dissolution cycle is superimposed on another time series, high production stands out as either spikes of $CaCO_3$ burial or low coherence with other records.

The large regional scale of the carbonate dissolution signal (and perhaps glacial increases in production, Hagelberg et al., 1995) imposes a basin-wide pattern of carbonate burial. Carbonate time series in eastern North Pacific cores have similarities to carbonate records in the equatorial Pacific with a 100 kyr cycle of dissolution and with high $CaCO_3$ dissolution in the interglacials (Fig 2; Zahn et al, 1991; Karlin et al, 1992; Lyle et al, 2000). If changes in dissolution were the major cause of the Site 882 record, the $CaCO_3$ record in the Kamchatka region of the NW Pacific would have a glacial peak of $CaCO_3$ deposition and not an early interglacial signal.

Jaccard et al (2005) produced biogenic barium (bio-Ba) records for Site 882 and show that bio-Ba peaks align with $CaCO_3$ peaks to the base of their record, through MIS-11 ~420 ka. High Ba flux is correlated with high POC flux falling to the seafloor (Dymond et al, 1992), so there is an implication that high productivity caused high $CaCO_3$ MAR. However, not all bio-Ba peaks are $CaCO_3$ peaks. Jaccard et al (2009) only archived part of the bio-Ba data, for the last 150 kyr, which we have plotted both as wt% data and MAR against the other biogenic records (Fig 6) using the age model from this paper. Jaccard et al (2005, 2009) found that major bio-Ba increases occur in tandem with the $CaCO_3$ deposition. However, Ba MAR best resembles a combined bio-SiO_2 and $CaCO_3$ record, indicating that changes in primary productivity only partly shaped the $CaCO_3$ record. Other factors determined when high amounts of $CaCO_3$ were produced.

Jaccard et al. (2009) also argue, based on redox sensitive elements, that glacial deep waters in the NW Pacific were oxygen-depleted, but were rapidly oxygenated during the deglaciation. Jaccard et al (2009) also proposed that the lack of $CaCO_3$ deposition in glacial intervals was caused by undersaturation of $CaCO_3$ during the low oxygen intervals and complete dissolution of $CaCO_3$ at the sea floor. However, good preservation of $CaCO_3$ in glacial intervals along North Pacific Deep Water (NPDW) flowlines in the eastern North Pacific (Fig 2) indicates that the lack of $CaCO_3$ in glacial intervals at Site 882 and the Kamchatka margin was not caused by higher abyssal dissolution in glacial intervals. Deep water flows from the Antarctic into the western North Pacific and exits east of Hawaii, generally near the Americas (Figure 1B). Note that Deep water flowing from the Antarctic across the Ontong Java Plateau in the southwest Pacific caused less dissolution in glacial intervals versus the interglacials (Site 805, 3200m, Yasuda et al, 1995; Site 807, 2805 m, Zhang et al., 2007). This pattern of dissolution is also characteristic of Shatsky Rise, at ~30° N, ~20° south of the Kamchatka margin (Site 1209, 2387 m Bordiga et al., 2013), and characteristic of the northeast Pacific and equatorial Pacific (Figure 2, Farrell and Prell, 1989; Zahn et al,

https://doi.org/10.5194/egusphere-2026-3515
Preprint. Discussion started: 26 August 2026

1991; Karlin et al, 1992; Lyle et al, 2000). Therefore, Deep water flowing into the NW Pacific toward Site 882 should not be more corrosive during the Pleistocene glacial intervals because the deep water elsewhere in the Pacific caused better $CaCO_3$ preservation. A shift of NPDW to deeper levels during glacials (Knudsen and Ravelo, 2015) might shift the O_2 minimum to be at Site 882 depth but should not strongly affect carbonate preservation.

The conversion of wt% data to MAR in Figure 5 weakens the antithetical relationship between bio-Ba and POC in MIS 5. The low sedimentation rate at the beginning of MIS 5 most probably results from lower clay deposition offshore as the clay source regions on the Kamchatka margin are submerged. Decreased burial of POC at the beginning of the Holocene and during the MIS 5 interglacial interval supports the hypothesis of Jaccard et al (2009) of a change in oxygenation from poorly oxygenated with better POC preservation to much more oxygenated deep waters and reduced POC burial. Low POC relative to Ba has also been used to indicate poor POC preservation in the Eocene and in the early Miocene in the equatorial Pacific (Olivarez Lyle and Lyle, 2006; Lyle and Olivarez Lyle, 2024). A rebound of the oxygen minimum to shallower depths and increased Holocene flow of oxygenated deep water from the Antarctic may explain the POC data, but the bio-Ba should result from the combined flux of rain from phytoplankton that produce $CaCO_3$ to those that produce bio-SiO_2.

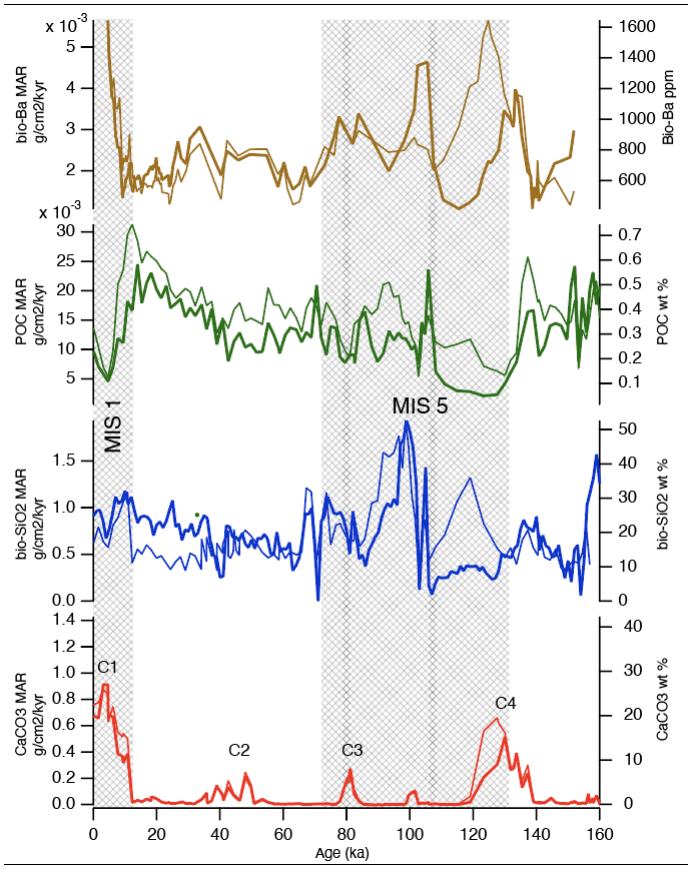

https://doi.org/10.5194/egusphere-2026-3515
Preprint. Discussion started: 26 August 2026

Figure 6: Biogenic time series of the last 160 kyr, including the bio-Ba time series from Jaccard et al (2009). Thick lines are MAR, while thin lines are wt % or ppm. MAR values better align than percentage data, because high percentages around 120 ka are associated with low sedimentation rates and possibly less clay burial.

The biogenic evidence suggests that nutrients begin to be delivered to surface waters to enhance diatom production within the MIS 5 deglaciation, at the beginning of the bio-Ba increase. However, as the deglaciation progressed, upwelling becomes weaker and nutrient transport lessened to favor coccolithophorid production over diatoms and weakened transport of POC to the sea floor (Ravelo et al, 1997, Rykaczewski and Checkley, 2008). In the modern ocean, this can be seen by changes in bio-SiO_2/$CaCO_3$ ratios caught in sediment traps across a NE Pacific upwelling zone (Dymond and Lyle, 1994) as productivity decreases offshore. The sediment trap in a deployment 100 km from the coast (the "*Nearshore"* trap deployment) measured bio-SiO_2 /$CaCO_3$ caught in near-bottom sediment traps of 3.23, while this ratio farther from shore (270 km; the "*Midway"* traps) was 1.82, 70% less than the *Nearshore* location. Furthermore, the POC rain decreased by more than a factor of two from "*Nearshore"* to "*Midway*". Further destruction of POC occurred when the bottom waters flowing over Site 882 became more oxygenated during deglaciations, leading to the low POC burial associated with the early interglacial $CaCO_3$ intervals.

4.2 What the Site 882 alkenone records reveal

For Site 882, Haug (1995) derived alkenone sea surface temperature (SST) records for the last 4 million years, and subsequently, Martinez-Garcia et al. (2010) analysed what appears to be the same samples from 3.65 Ma to the present for the 4-unsaturated C37 alkenone ($C_{37:4}$) relative abundance. The presence of alkenones in both glacial and interglacial intervals demonstrates that coccolithophorids were present throughout the Pleistocene, even though $CaCO_3$ is only intermittently found in the record. Unfortunately, total abundance of the alkenones at Site 882 was not reported by either Haug (1995) or Martinez-Garcia, 2010) thus precluding an evaluation of coccolithophorid abundances during intervals when $CaCO_3$ was not preserved. High alkenone content and no $CaCO_3$ would be a strong indicator that carbonate dissolution defined the $CaCO_3$ profile.

4.2.1 Alkenone $C_{37:4}$ records and the presence of cold low salinity waters

High abundance of the $C_{37:4}$ alkenone fraction is correlated with both cold and less-saline waters in the Norwegian Sea (<5°C, < ~32 psu; Rosell-Melee, 1998; Bendle, 2005). The alkenone SST curve and the $C_{37:4}$ profiles are shown with the $CaCO_3$ profile in Figure 7, where significant $CaCO_3$ intervals have been numbered as in Table 1. $C_{37:4}$ is more highly expressed than are the other haptophyte alkenones in cold, low salinity water where sea ice is prevalent in the Norwegian Sea (Bendle et al, 2005). They also found that the relationship may be somewhat different than in the Bering Sea, although still correlated to surface salinity (Harada et al., 2003). At Site 882, Martinez-Garcia et al (2010) examined the $C_{37:4}$ trend since the late Pliocene and found major increases after 1.2 Ma, indicative of the expansion of cold, low salinity polar water at that time.

https://doi.org/10.5194/egusphere-2026-3515
Preprint. Discussion started: 26 August 2026

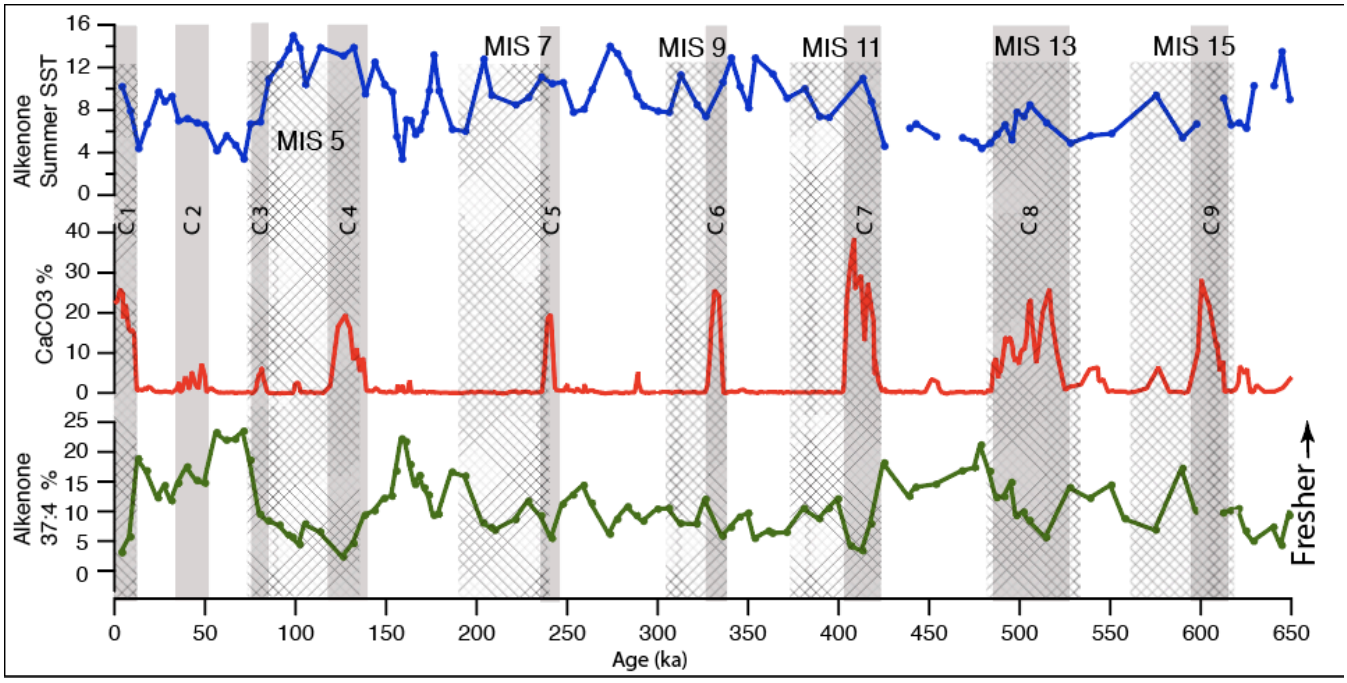

Figure 7: Alkenone evidence for surface ocean conditions during Pleistocene high $CaCO_3$ intervals (data from Haug,1995, and Martinez-Garcia et al., 2010). The high $CaCO_3$ intervals tend to fall within locally high summer SST but not necessarily the warmest SST. High $CaCO_3$ intervals all fall in intervals of higher salinity. Note that the peak of interval C6 and C9 are not sampled. MIS interglacials are shown with diamond hatching.

When the Site 882 data are plotted over the last 650 kyr, there is trend where low C37:4 intervals (higher salinity reflecting open North Pacific conditions) correlate with high $CaCO_3$ deposition. Two intervals of high $CaCO_3$ deposition (C6 and C9) are missing 37:4 alkenone data at peak deposition and were sampled on the flanks of the interval but not during peak $CaCO_3$ burial. Both $CaCO_3$ and bio-Ba deposition are associated with more saline waters of the North Pacific rather than the sea-ice rich, low salinity waters from the Bering Sea and Sea of Okhotsk. The 37:4 alkenone data fits with observations of sea-ice diatoms for the last 180 kyr in a core nearby to Site 882, MD01-2416 (Ren, 2015). Ren observed sea ice diatoms during MIS 6 from the base of his record to122 ka, and between 108 and 14 ka. The sea ice diatoms appear during periods of low $CaCO_3$ content and not in peak $CaCO_3$ intervals C1 and C4 (Fig 7).

4.2.2 The alkenone record and SST over the last 650 kyr

In the eastern North Pacific along the California Margin, Lyle et al, (2000) found the glacial intervals are more carbonate-rich and that high $CaCO_3$ intervals within the glacial intervals have a productivity component. During glacial intervals MIS 2-3-4 and MIS 6, the base level $CaCO_3$ burial rates fit with the dissolution model of $CaCO_3$ preservation. However, occasional high

https://doi.org/10.5194/egusphere-2026-3515
Preprint. Discussion started: 26 August 2026

$CaCO_3$ intervals have more $CaCO_3$ deposited than that of the modern rain through the water column caught by sediment traps. A significant increase in $CaCO_3$ production must have occurred at those times. High $CaCO_3$ deposition occurs now in sites offshore in the subarctic North Pacific where February SST is around 7-9°C and September SST is around 14-16°C. One hypothesis from that observation is that moderate winter SST and relatively warm summer/fall SST produces conditions that maximize $CaCO_3$ production.

The alkenone SST at Site 882 most likely represents a summer SST (Meheust et al., 2013). For example, the youngest alkenone estimated SST should represent modern conditions. However, SST that high is reached only during peak summer—August and September (Station 50N, Onodera et al, 2005). Similarly, alkenone SST is a record of autumn temperatures in the sea of Okhotsk (Harada et al, 2006) where autumn is found to be the season of the highest coccolithophorid E. *huxleyi* production. The data from Martinez-Garcia et al. (2010) also shows that warm SST intervals have low $C_{37:4}$ contents, indicating lower proportions of cold low salinity water.

Although high $CaCO_3$ sediments tend to be deposited during warm SST intervals at Site 882, not all warm intervals are high in $CaCO_3$. Highest temperatures in the last 650 kyr occur in the MIS 6/5 interval, between 153 ka and 85 ka. Since the ages straddle the peak glacial MIS 6 through much of the MIS 5 interglacial, high summer SST clearly results from more than high northern summer insolation but probably includes advection of warm (or cold) surface waters to the site, or stabilization of a thin surface layer to be heated by solar insolation. The poorly sampled C6 and C9 high $CaCO_3$ intervals do not have a SST peak perhaps because peak $CaCO_3$ deposition was not sampled by Haug (1995).

The situation at Site 882 is different than for sites along the California margin (Lyle et al., 2000), where peak glacial carbonate deposition is larger than the modern carbonate rain and peaked at 16.6 ka in the late glacial interval. In the Holocene, $CaCO_3$ is almost absent from Holocene California margin sediments. The NE Pacific deglacial $CaCO_3$ peak occurred because of a combination of better preservation at the sea floor, more diffuse upwelling that favored coccolithophorid production, and optimum conditions for coccolithophorid growth. At Site 882 off the Kamchatka margin, replacement of low salinity waters by waters sourced in the North Pacific gyre are probably more important than warm SST. High summer SST at Site 882, even within glacial intervals, possibly reflects lower mixing when low salinity surface waters are present.

4.3 Sea ice around Site 882 in glacial intervals as a factor in $CaCO_3$ production

Evidence exists that ice was present around Site 882 for at least the last glacial interval. Glacial sediments contain sea-ice diatoms and sea-ice biomarkers showing that some sea ice was present off the Kamchatka margin. Few studies have extended earlier than 125 ka, so little data exists for sea ice in earlier glacial intervals. We propose that sea ice, and/or the low salinity

https://doi.org/10.5194/egusphere-2026-3515
Preprint. Discussion started: 26 August 2026

surface water that accompanies sea ice, probably was present as far east as Detroit Seamount (Site 882) in previous Pleistocene glacial intervals since 650 ka.

Sea ice proxies are found off the Kamchatka margin during the last glacial interval (Max et al., 2012; Meheust et al., 2014; Ren, 2015; Meheust et al., 2016) but not in Holocene sediments (Sancetta, 1983; Ren et al., 2014; Meheust et al., 2013). Presence of sea ice within a region should indicate a region of lower surface salinity and stronger pycnocline, isolating the surface layer from mixing with nutrient-rich waters below. However, there is not a strong presence of sea ice proxies in glacials that could be interpreted as evidence for major winter sea ice cover. Based on the Caissie et al. (2010) calibration, the level of *Fragilariopsis* spp found in the Detroit Seamount core MD01-2416 is equivalent to <1 month/yr of sea ice cover, and Ren et al (2014) suggest that the concentration of *Fragilariopsis* spp found downcore can be found in the open ocean up to 300 km from the modern winter sea ice edge. Nevertheless, we know that the western Bering Sea to the north, now with ice cover only during the winter ice maximum, was probably covered by sea ice during glaciations. In addition, the Okhotsk Sea was probably ice covered at least up to the slope break (Max et al., 2012). If the ice edge moved southward and westward in the Bering Sea, and east in the Okhotsk Sea, low salinity surface water with some sea ice probably found its way into the Western Subarctic gyre where Site 882 is found. Currents from the edge of sea-ice probably also carried some sea ice to the vicinity of Site 882.

We know that low salinity surface water was found over Detroit Seamount for most glacial intervals based on alkenones (Fig 7, Martinez-Garcia et al, 2010) and based on a diatom characteristic of low salinity subpolar water in a core adjacent to Site 882 (*T. trifulta*, Sancetta, 1983). In core MD-01-2416, also on the Detroit Seamount, the diatom was present throughout the glacial stages since 180 ka (Ren, 2015). The carbonate records would suggest that a relatively low surface salinity layer was only briefly replaced early in interglacial intervals by more saline waters characteristic of the open North Pacific, when conditions were conducive to high carbonate production. We propose that the relatively high salinity water is found in the Detroit Seamount region when the Bering Strait opened to the Arctic Ocean. Fresher water would then have flowed northward and transported out of the Bering Sea into the Arctic and eventually to the North Atlantic. In other words, the opening allowed more saline Pacific seawater to flow northward into the Western Subarctic Gyre of the North Pacific where Site 882 is located (Fig 2).

4.3 Evidence from the last deglaciation along the Kamchatka margin

On the MIS2/1 deglaciation, the beginning $CaCO_3$ accumulation at Site 882 occurs between 12.3 and 10.8 ka. A similar deglacial rise in $CaCO_3$ is found in piston cores from the Kamchatka region on Meiji Seamount (Keigwin et al, 1992; Keigwin, 1998) although the $CaCO_3$ rise is dated somewhat earlier, ~12.6 ka. The early part of the $CaCO_3$ interval is also associated with a minor high bio-SiO_2 interval (Figs. 5 and 6), evidence of an early Holocene productivity rebound around the Bering Sea (Pelto et al, 2018) that ended soon after the Bering Strait flooded. The evidence from the last deglaciation suggests that the

https://doi.org/10.5194/egusphere-2026-3515
Preprint. Discussion started: 26 August 2026

high $CaCO_3$ interval is associated with the development of an ocean connection between the North Pacific and Arctic Ocean. Higher salinity waters from the Alaska Gyre could then cover the Site 882 region as water from the Bering Sea was diverted northward. Other dynamics may have been involved; however, the age model is not sufficiently robust to definitively link the $CaCO_3$ burial intervals to the North Pacific-Arctic linkage. Nevertheless, the $CaCO_3$ burial intervals began late in the deglaciation and are associated with profound northern climate change.

We have little information about the Bering Strait for earlier deglaciations, yet high $CaCO_3$ seems to be associated with a sea level rise that connects the Pacific and Arctic Oceans. In Figure 3 we compare the Spratt and Lisiecki (2016) stacked late Pleistocene sea-level record to our $CaCO_3$ data at Site 882 to examine the relationship between $CaCO_3$ depositional intervals to changes in global mean sea level. There is a strong association with the time of high $CaCO_3$ burial and the rapid rise of sea level; particularly when sea level breaches the depth of the Bering Strait. The extensive $CaCO_3$ deposition in the C8 interval (525-481 ka) occurs during a time when sea level hovered near the Bering Strait sill depth so also supports the hypothesis that diversion of fresher waters into the Arctic may have promoted $CaCO_3$ burial along the Kamchatka margin. However, we note that $CaCO_3$ deposition was not strictly dependent upon sea level rising above the sill depth, (e.g., the C2 interval between 51 and 32 ka, Figure 3, Table 1) and suggest that other factors promoted or depressed $CaCO_3$ production and preservation in the NW Pacific.

5 Conclusions

Cores near the Kamchatka margin of the NW Pacific have $CaCO_3$ time series different than cores within deep waters flowing into the deep North Pacific (Yasuda et al, 1995, Zhang et al., 2007) and those at the same depth exiting the region (Farrell and Prell, 1989; Lyle et al, 2000; Lyle et al., 2019). Jaccard et al. (2009) argued that the $CaCO_3$ time series was caused by dissolution from the high DIC and low O_2 deep waters that bathed Detroit Seamount during glacial intervals. We conclude, in contrast to a dissolution signal, that the $CaCO_3$ sedimentary record reflects higher production in surface waters when higher salinity waters occupied the surface above Site 882 and when there was better $CaCO_3$ production by coccolithophorids. When the rest of the Pacific experienced higher $CaCO_3$ burial during glacials, $CaCO_3$ production at Site 882 was suppressed by a low salinity surface layer containing some sea ice. Higher salinity waters, more conducive to $CaCO_3$ production, occupied the region when rising sea level flooded the Bering Strait; allowing water passage into the Arctic Ocean, and for low salinity surface water to exit the Bering Sea to the north. While we have emphasized the opening of the Bering Strait, there are likely other factors that led to higher salinity, more $CaCO_3$ productive surface waters to appear at the beginnings of interglacial intervals. The high coccolithophorid production led to peaks in bio-Ba deposition (Jaccard et al, 2005). The consistent relationship between high $CaCO_3$ intervals and flooding of the Bering Strait for the past 650 kyr demonstrates a common response of the Kamchatka margin to Pleistocene glacial cycles.

https://doi.org/10.5194/egusphere-2026-3515
Preprint. Discussion started: 26 August 2026

6 Code/Data Availability

Site 882 was re-correlated into a continuous sediment section using the *Code for Ocean Drilling Data* package (https://www.codd-home.net/; Wilkens et al., 2017) which allowed us to also splice core images and to check the splicing (see Supplemental Material). All data for this project are being archived at Pangaea.de (doi: **not submitted yet**).

7 Author Contributions

ML noted the difference in carbonate profiles for the NW Pacific and designed the potential test. ML also had primary responsibility for writing the paper. AOL was responsible for data analysis and quality control of the data. AOL also critiqued the ideas and helped with writing and editing.

8 References

Abdul, N. A., Mortlock, R. A., Wright, J. D., and Fairbanks, R. G.: Younger Dryas sea level and meltwater pulse 1B recorded in Barbados reef crest coral Acropora palmata, Paleoceanography, 31, 330-344, 10.1002/2015PA002847, 2016.

Arrhenius, G. O. S.: Sediment cores from the east Pacific,, in: Reports of the Swedish Deep Sea Expedition, 1947-1948, 5, 1-228, 1952.

Bendle, J., Rosell-Mele, A., and Ziveri, P.: Variability of unusual distributions of alkenones in the surface waters of the Nordic seas, Paleoceanography, 20, PA2001, 10.1029/2004PA001025, 2005.

Bordiga, M., Beaufort, L., Cobianchi, M., Lupi, C., Mancin, N., Luciana, V., Pelosi, N., and Sprovieri, M.: Calcareous plankton and geochemistry from the ODP site 1209B in the NW Pacific Ocean (Shatsky Rise): New data to interpret calcite dissolution and paleoproductivity changes of the last 450 ka, Palaeogeography, Palaeoclimatology, Palaeoecology, 371, 93-108, http://dx.doi.org/10.1016/j.palaeo.2012.12.021, 2013.

Caissie, B. E., Brigham-Grette, J., Lawrence, K. T., and Herbert, T. D.: Last Glacial Maximum to Holocene sea surface conditions at Umnak Plateau, Bering Sea, as inferred from diatom, alkenone, and stable isotope records, Paleoceanography, 25, PA1206, 10.1029/2008PA001671, 2010.

Cessi, P.: Control of Bering Strait Transport by the Meridional Overturning Circulation, Journal of Physical Oceanography 50, 1853-1870, 2020.

Conte, M. H., Ralph, N., and Ross, E. H.: Seasonal and interannual variability in deep ocean particle #uxes at the Oceanic Flux Program (OFP)/Bermuda Atlantic Time Series (BATS) site in the western Sargasso Sea near Bermuda, Deep Sea Research II, 48, 1471-1505, 2001.

Dymond, J. and Lyle, M.: Flux comparisons between sediments and sediment traps in the eastern tropical Pacific: Implications for atmospheric CO2 variations during the Pleistocene, Limnology and Oceanography, 30, 699-712, 1985.

Dymond, J., Suess, E., and Lyle, M.: Barium in deep-sea sediment: A geochemical proxy for paleoproductivity, Paleoceanography, 7, 163-181, 1992.

https://doi.org/10.5194/egusphere-2026-3515
Preprint. Discussion started: 26 August 2026

Dymond, J. and Lyle, M.: Particle fluxes in the ocean and implications for sources and preservation of ocean sediments, in: Material Fluxes on the Surface of the Earth, edited by: Hay, W. W., Andrews, J. T., Baker, V. R., Dymond, J., Kump, L. R., Lerman, A., Martin, W. R., Meybeck, M., Milliman, J. D., Rea, D. K., and Sayles, F. L., National Academy Press, Washington DC, 125-143, 1994.

Farrell, J. W. and Prell, W. L.: Climatic change and CaCO3 preservation: an 800,000 year bathymetric reconstruction from the central equatorial Pacific Ocean, Paleoceanography, 4, 447-466, 1989.

Hagelberg, T. K., Pisias, N. G., Mayer, L. A., Shackleton, N. J., and Mix, A. C.: Spatial and temporal variability of late Neogene equatorial Pacific Carbonate: Leg 138, in: Proceedings of the Ocean Drilling Program, Scientific Results, edited by: Pisias, N. G., Mayer, L. A., Janecek, T. R., Palmer-Julson, A., and van Andel, T. H., Ocean Drilling Program, College Station, TX, 321-336, 1995.

Harada, N., Shin, K. H., Murata, A., Uchida, M., and Nakatani, T.: Characteristics of alkenones synthesized by a bloom of Emiliania huxleyi in the Bering Sea, Geochimica et Cosmochimica Acta, 67, 1507-1519, 2003.

Harada, N., Ahagon, N., Sakamoto, T., Uchida, M., Ikehara, M., and Shibata, Y.: Rapid fluctuation of alkenone temperature in the southwestern Okhotsk Sea during the past 120 ky, Global and Planetary Change, 53, 29-46, 2006.

Haug, G. H.: Zur Paleo-Ozeanographie und Sedimentationsgeschichte im Nordwest-Pazifik w√§hrend der letzten 6 Millionen Jahre (ODP-Site 882). Mathematisch-Naturwissenschaftliche Fakult, Christian-Albrechts-Universitat zu Kiel, Kiel Germany, 98 pp., 1995.

Haug, G. H., Maslin, M. A., Sarnthein, M., Stax, R., and Tiedemann, R.: Evolution of northwest Pacific sedimentation patterns since 6 Ma (Site 882), in: Proceedings of the Ocean Drilling Program, Scientific Results, edited by: Rea, D. K., Basov, I. A., Scholl, D. W., and Allan, J. F., Ocean Drilling Program, College Station TX, 293-315, 1995.

Haug, G. H., Sigman, D. M., Tiedemann, R., Pedersen, T. F., and Sarnthein, M.: Onset of permanent stratification in the subarctic Pacific Ocean, Nature, 401, 779-782, 1999.

Hays, J. D., Saito, T., Opdyke, N. D., and Burckle, L. H.: Pliocene-Pleistocene sediments of the equatorial Pacific: Their paleomagnetic, biostratigraphic, and climatic record, Geological Society of America Bulletin, 80, 1481-1514, 1969.

Honda, M. C., Imai, K., Nojiri, Y., Hoshi, F., Sugawara, T., and Kusakabe, M.: The biological pump in the northwestern North Pacific based on fluxes and major components of particulate matter obtained by sediment-trap experiments (1997-2000), Deep Sea Research II, 49, 5595-5625, 2002.

Honjo, S., Dymond, J., Collier, R., and Manganini, S. J.: Export production of particles to the interior of the equatorial Pacific Ocean during the 1992 EqPac experiment, Deep-Sea Research II, 42, 831-870, 1995.

Honjo, S., Dymond, J., Prell, W. L., and Ittekkot, V.: Monsoon-controlled export fluxes to the interior of the Arabian Sea, Deep Sea Research II, 46, 1859-1902, 1999.

Hu, A., Meehl, G. A., Otto-Bliesner, B. L., Waelbroeck, C., Han, W., Loutre, M.-F., Lambeck, K., Mitrovica, J. X., and Rosenbloom, N.: Influence of Bering Strait flow and North Atlantic circulation on glacial sea-level changes, Nature Geoscience, 3, 118-121, 2010.

Hu, A., Meehl, G. A., Han, W., Otto-Bliesner, B. L., and Abe-Ouchi, A.: Effects of the Bering Strait closure on AMOC and global climate under different background climates, Progress in Oceanography, 132, 174-196, http://dx.doi.org/10.1016/j.pocean.2014.02.004, 2015.

Jaccard, S. L., Haug, G. H., Sigman, D. M., Pedersen, T. F., Thierstein, H. R., and Röhl, U.: Glacial/Interglacial Changes in Subarctic North Pacific Stratification, Science, 308, 1003-1006, 2005.

https://doi.org/10.5194/egusphere-2026-3515
Preprint. Discussion started: 26 August 2026

Jaccard, S. L., Galbraith, E. D., Sigman, D. M., Haug, G. H., Francois, R., Pedersen, T. F., Dulski, P., and Thierstein, H. R.: Subarctic Pacific evidence for a glacial deepening of the oceanic respired carbon pool, Earth and Planetary Science Letters, 277, 156-165, 2009.

Jaccard, S. L., Galbraith, E. D., Sigman, D. M., and Haug, G. H.: A pervasive link between Antarctic ice core and subarctic Pacific sediment records over the past 800 kyrs, Quaternary Science Reviews, 29, 206-2012, 2010.

Jakobbson, M., Pearce, C., Cronin, T. M., Backman, J., Anderson, L. G., Barrientos, N., Björk, G., Coxall, H. K., de Boer, A. M., Mayer, L. A., Möerh, C.-M., Nilsson, J., Rattray, J. E., Stranne, C., Semiletov, I., and O'Regan, M.: Post-glacial flooding of the Bering Land Bridge dated to 11 cal kaBP based on new geophysical and sediment records, Climate of the Past, 13, 991-1005, 10.5194/cp-13-991-2017, 2017.

Karlin, R., Lyle, M., and Zahn, R.: Carbonate variations in the northeast Pacific during the Late Quaternary, Paleoceanography, 7, 43-63, 1992.

Kawabe, M. and Fujio, S.: Pacific Ocean circulation based on observation, Journal of Oceanography, 66, 389-403, 2010.

Keigwin, L. D., Jones, G. A., and Froelich, P. N.: A 15,000 year paleoenvironmental record from Meiji Seamount, far northwestern Pacific, Earth and Planetary Science Letters, 111, 425-440, 1992.

Keigwin, L. D.: Glacial-age hydrography of the far northwest Pacific Ocean, Paleoceanography, 13, 323-339, 1998.

Knudson, K. P. and Ravelo, A. C.: North Pacific Intermediate Water circulation enhanced by the closure of the Bering Strait, Paleoceanography, 30, 1287-1304, 10.1002/2015PA002840, 2015.

Kotilainen, A. T. and Shackleton, N. J.: Rapid climate variability in the North Pacific Ocean during the past 95,000 years, Nature, 377, 323-326, 1995.

Lisiecki, L. E. and Raymo, M. E.: A Pliocene-Pleistocene stack of 57 globally distributed benthic d18O records, Paleoceanography, 20, PA1003, 10.1029/2004PA001071, 2005.

Lyle, M., Mix, A., Ravelo, C., Andreasen, D., Heusser, L., and Olivarez, A.: Millennial-scale CaCO3 and C-org events along the northern and central California margin: stratigraphy and origins, in: Proceedings of the Ocean Drilling Program, Scientific Results, 167, edited by: Lyle, M., Koizumi, I., Moore, T. C., jr., and Richter, C., Ocean Drilling Program, College Station TX, 163-182, 2000.

Lyle, M., Heusser, L. E., Ravelo, A. C., Andreasen, D., Olivarez Lyle, A., and Diffenbaugh, N.: Pleistocene water cycle and eastern boundary current processes along the California continental margin, Paleoceanography, 25, PA4211, 4219pp, 10.1029/2009PA001836, 2010.

Lyle, M. and Baldauf, J.: Biogenic sediment regimes in the Neogene equatorial Pacific, IODP Site U1338: Burial, production, and diatom community, Palaeogeography, Palaeoclimatology, Palaeoecology, 433, 106-128, 10.1016/j.palaeo.2015.04.001, 2015.

Lyle, M., Drury, A. J., Tian, J., Wilkens, R., and Westerhold, T.: Late Miocene to Holocene high-resolution eastern equatorial Pacific carbonate records: stratigraphy linked by dissolution and paleoproductivity, Climate of the Past, 15, 1715-1739, https://doi.org/10.5194/cp-15-1715-2019, 2019.

Lyle, M. and Olivarez Lyle, A., Variations in the biological pump throughout the Miocene: evidence from organic carbon burial in Pacific Ocean sediments, Clim. Past, 20, 2685–2700, https://doi.org/10.5194/cp-20-2685-2024, 2024

https://doi.org/10.5194/egusphere-2026-3515
Preprint. Discussion started: 26 August 2026

Martinez-Garcia, A., Rosell-Mele, A., McClymont, E. L., Gersonde, R., and Haug, G. H.: Subpolar Link to the Emergence of the Modern Equatorial Pacific Cold Tongue, Science, 328, 1550-1553, 10.1126/science.1184480, 2010.

Max, L., Riethdorf, J.-R., Tiedemann, R., Smirnova, M., Lembke-Jene, L., Fahl, K., Nürnberg, D., Matul, A., and Mollenhauer, G.: Sea surface temperature variability and sea-ice extent in the subarctic northwest Pacific during the past 15,000 years, Paleoceanography, 27, PA3213, 10.1029/2012PA002292,, 2012.

McClymont, E. L., Rosell-Mele, A., Haug, G. H., and LLoyd, J. M.: Expansion of subarctic water masses in the North Atlantic and Pacific oceans and implications for mid-Pleistocene ice sheet growth, Paleoceanography, 23, PA4214, 10.1029/2008PA001622, 2008.

Meheust, M., Fahl, K., and Stein, R.: Variability in modern sea surface temperature, sea ice and terrigenous input in the sub-polar North Pacific and Bering Sea: Reconstruction from biomarker data, Organic Geochemistry, 57, 54-64, 10.1016/j.orggeochem.2013.01.008, 2013.

Meheust, M., Stein, R., Fahl, K., Max, L., and Riethdorf, J.-R.: High-resolution IP25-based reconstruction of sea-ice variability in the western North Pacific and Bering Sea during the past 18,000 years, Geo-Marine Letters, 36, 101-111, 10.1007/s00367-015-0432-4, 2016.

Moriceau, B., Iversen, M. H., Gallinari, M., Evertsen, A.-J., Le Goff, M., Beker, B., Boutorh, J., Corvaisier, R., Coffineau, N., Lampitt, R. S., Le Mercier, A., Masson, A., Stibor, H., Stockenreiter, M., and De La Rocha, C. L.: Copepods Boost the Production but Reduce the Carbon Export Efficiency by Diatoms, Frontiers in Marine Science, 5, 10.3389/fmars.2018.00082, 2018.

Olivarez Lyle, A. and Lyle, M.: Determination of biogenic opal in pelagic marine sediments: a simple method revisited, in: Proceedings of the Ocean Drilling Program, Initial Reports Volume 199, edited by: Lyle, M., Wilson, P.A., Janecek, T.R., et al.,, Ocean Drilling Program, College Station TX, http://www-odp.tamu.edu/publications/199_IR/chap_106/chap_106.htm, 10.2973/odp.proc.ir.199.106.2002, 2002.

Olivarez Lyle, A. and Lyle, M.: Organic carbon and barium in Eocene sediments: Possible controls on nutrient recycling in the Eocene equatorial Pacific Ocean, in: Proceedings of the Ocean Drilling Program, Scientific Reports Volume 199, edited by: Lyle, M., Wilson, P.A., Janecek, T.R., et al.,, Ocean Drilling Program, College Station TX, 1-33; http://www-odp.tamu.edu/publications/199_IR/chap_106/chap_106.htm, 2005.

Olivarez Lyle, A. and Lyle, M.: Organic carbon and barium in Eocene sediments: Is metabolism the biological feedback that maintains end-member climates?, Paleoceanography, 21, 1-13; doi:10.1029/2005PA001230, 2006.

Onodera, J., Takahashi, K., and Honda, M. C.: Pelagic and coastal diatom fluxes and the environmental changes in the northwestern North Pacific during December 1997–May 2000, Deep Sea Research II, 52, 2218-2239, 10.1016/j.dsr2.2005.07.005, 2005.

Pelto, B. M., Caissie, B. E., Petsch, S. T., and Brigham-Grette, J.: Oceanographic and Climatic Change in the Bering Sea, Last Glacial Maximum to Holocene, Paleoceanography and Paleoclimatology, 33, 93-111, 10.1002/2017PA003265, 2018.

Pico, T., Mitrovica, J. X., and Mix, A. C.: Sea level fingerprinting of the Bering Strait flooding history detects the source of the Younger Dryas climate event, Science Advances, 6, 10.1126/sciadv.aay2935, 2020.

Ragueneau, O., Tréguer, P., Anderson, R. F., Brzezinski, M. A., DeMaster, D. J., Dugdale, R. C., Dymond, J., Fischer, G., François, R., Heinze, C., Leynaert, A., Maier-Reimer, E., Martin-Jézéquel, V., Nelson, D. M., and Quéguiner, b.: A review of the Si cycle in the modern ocean; recent progress and missing gaps in the application of biogenic opal as a paleoproductivity proxy, Global and Planetary Change, 26, 317-365, 2000.

https://doi.org/10.5194/egusphere-2026-3515
Preprint. Discussion started: 26 August 2026

Ravelo, A. C., Lyle, M., Koizumi, I., Caulet, J. P., Fornaciari, E., Hayashida, A., Heider, F., Hood, J., Hovan, S., Janecek, T., Janik, A., Stax, R., Yamamoto, M., and Party, O. L. S.: Pliocene carbonate accumulation along the California margin, Paleoceanography, 12, 729-741, 1997.

Ren, J., Gersonde, R., Esper, O., and Sancetta, C.: Diatom distributions in northern North Pacific surface sediments and their relationship to modern environmental variables, Palaeogeography, Palaeoclimatology, Palaeoecology, 402, 81–103, 2014.

Ren, J.: Late Pleistocene paleoceanography of the Subarctic Pacific derived from the diatom record, Fachbereich Geowissenschaften, Universität Bremen, 141 pp., 2015.

Rosell-Mele, A.: Interhemispheric appraisal of the value of alkenone indices as temperature and salinity proxies in high-latitude locations, Paleoceanography, 13, 694-703, 1998.

Rykaczewski, R. R. and Checkley, D. M. j.: Influence of ocean winds on the pelagic ecosystem in upwelling regions, Proceedings of the National Academy of Science, 105, 1965-1970, 10.1073_pnas.0711777105, 2008.

Samtleben, C., Schafer, P., Andruleit, H., Baumann, A., Baumann, K.-H., Kohly, A., Matthiessen, J., Schroder-Ritzrau, and 'Synpal'Working group: Plankton in the Norwegian-Greenland Sea: from living communities to sediment assemblages an actualistic approach, Geologisch Rundschau, 84, 108-136, 1995.

Sancetta, C.: Effect of Pleistocene glaciation upon oceanographic characteristics of the North Pacific Ocean and Bering Sea, Deep-Sea Research, 30, 851-869, 1983.

Spratt, R. M. and Lisiecki, L. E.: A Late Pleistocene sea level stack, Climate of the Past, 12, 1079-1092, 10.5194/cp-12-1079-2016, 2016.

Talley, L.D. (Ed.): Hydrographic Atlas of the World Ocean Circulation Experiment (WOCE): Volume 2: Pacific Ocean, International WOCE Project Office, Southampton, UK, 2007.
https://doi.org/10.21976/C6WC77

Talley, L. D., Pickard, G. L., Emery, W. L., and Swift, J. H.: Descriptive Physical Oceanography: an introduction (6th edition, 6th edition, Academic press, Amsterdam, 2011.

Tiedemann, R. and Haug, G. H.: Astronomical calibration of cycle stratigraphy for Site 882 in the northwest Pacific, in: Proceedings of the Ocean Drilling Program, Scientific Results, edited by: Rea, D. K., Basov, I. A., Scholl, D. W., and Allan, J. F., Ocean Drilling Program, College Station TX, 283-293, 1995.

Treguer, P., Bowler, C., Moriceau, B., Dutkiewicz, S., Gehlen, M., Aumont, O., Bittner, L., Dugdale, R. C., Finkel, Z., Iudicone, D., Jahn, O., Guidi, L., Lasbleiz, M., Leblanc, K., Levy, M., and Pondaven, P.: Influence of diatom diversity on the ocean biological carbon pump, Nature Geoscience, 11, 27-37, 10.1038/s41561-017-0028-x, 2018.

Wilkens, R., Westerhold, T., Drury, A. J., Lyle, M., Gorgas, T., and Tian, J.: Revisiting the Ceara Rise, equatorial Atlantic Ocean: isotope stratigraphy of ODP Leg 154 from 0 to 5 Ma, Climate of the Past, 13, 779-793, 10.5194/cp-13-779-2017, 2017.

Wong, C. S. and Crawford, D. W.: Flux of particulate inorganic carbon to the deep subarctic Pacific correlates with El Ni*no, Deep Sea Research II, 49, 5705-5715, 2002.

Woodgate, R. A.: Increases in the Pacific inflow to the Arctic from 1990 to 2015, and insights into seasonal trends and driving mechanisms from year-round Bering Strait mooring data, Progress in Oceanography, 160, 124-154, 2018.

https://doi.org/10.5194/egusphere-2026-3515
Preprint. Discussion started: 26 August 2026

Woodgate, R. A. and Aagaard, K.: Revising the Bering Strait freshwater flux into the Arctic Ocean, Geophysical Research Letters, 32, L02602, 10.1029/2004GL021747, 2005.

Yang, X. and Cessi, P.: The Bering Strait Throughflow Component of the Global Mass, Heat and Freshwater Transport, Journal of Geophysical Research: Oceans,, 129, e2024JC021463, https://doi.org/10.1029/2024JC021463, 2024.

Yasuda, M., Berger, W. H., Wu, G., Burke, S., and Schmidt, H.: Foraminifer preservation record for the last million years, Site 805, Ontong Java Plateau, in: Proceedings of the Ocean Drilling Program, Scientific Results, edited by: Berger, W. H., Kroenke, L. W., and Mayer, L. A., Ocean Drilling Program, College Station TX, 491-508, 1993.

Zahn, R., Pedersen, T. F., Bornhold, B. D., and Mix, A. C.: Water mass conversion in the glacial subarctic Pacific (54°N, 148°W): physical constraints and the benthic-planktonic stable isotope record, Paleoceanography, 6, 543-560, 1991.

Zhang, J., Wang, P., Li, Q., Cheng, X., Jin, H., and Zhang, S.: Western equatorial Pacific productivity and carbonate dissolution over the last 550 kyr: Foraminiferal and nannofossil evidence from ODP Hole 807A, Marine Micropaleontology, 64, 121-140, 10.1016/j.marmicro.2007.03.003, 2007.